

# Perception-in-the-Loop Adversarial Examples

Mahmoud Salamati  
MPI-SWS  
msalamati@mpi-sws.org

Sadegh Soudjani  
Newcastle University  
Sadegh.Soudjani@newcastle.ac.uk

Rupak Majumdar  
MPI-SWS  
rupak@mpi-sws.org

**Abstract**—We present a scalable, black box, perception-in-the-loop technique to find adversarial examples for deep neural network classifiers. Black box means that our procedure only has input-output access to the classifier, and not to the internal structure, parameters, or intermediate confidence values. Perception-in-the-loop means that the notion of proximity between inputs can be directly queried from human participants rather than an arbitrarily chosen metric. Our technique is based on covariance matrix adaptation evolution strategy (CMA-ES), a black box optimization approach. CMA-ES explores the search space iteratively in a black box manner, by generating populations of candidates according to a distribution, choosing the best candidates according to a cost function, and updating the posterior distribution to favor the best candidates. We run CMA-ES using human participants to provide the fitness function, using the insight that the choice of best candidates in CMA-ES can be naturally modeled as a perception task: pick the top  $k$  inputs perceptually closest to a fixed input.

We empirically demonstrate that finding adversarial examples is feasible using small populations and few iterations. We compare the performance of CMA-ES on the MNIST benchmark with other black-box approaches using  $L_p$  norms as a cost function, and show that it performs favorably both in terms of success in finding adversarial examples and in minimizing the distance between the original and the adversarial input. In experiments on the MNIST, CIFAR10, and GTSRB benchmarks, we demonstrate that CMA-ES can find perceptually similar adversarial inputs with a small number of iterations and small population sizes when using perception-in-the-loop. Finally, we show that networks trained specifically to be robust against  $L_\infty$  norm can still be susceptible to perceptually similar adversarial examples. Overall, we demonstrate that adversarial examples can be constructed in a black box way through direct human interaction.

**Index Terms**—Adversarial examples, deep neural networks, perception-in-the-loop, CMA-ES.

## I. INTRODUCTION

It is well known by now that deep neural networks are susceptible to *adversarial examples*: given an input, one can add a small perturbation to produce a new, perceptually similar, input that is classified differently but with high confidence (e.g. [11], [27]). Adversarial examples exist across many different domains and can be reproduced in physical artifacts. Not only do adversarial examples exist, they can be found comparatively easily through many different techniques, even when access to the classifier is limited to a black box setting. Clearly, they give rise to immediate safety and security concerns. Understanding the scope and prevalence of adversarial inputs, leading to their mitigation, is therefore a key challenge facing the deployment of DNNs in security or safety critical domains.

A key implicit assumption in an adversarial example is that the resulting input is *perceptually identical* to the original input. Indeed, in many situations, one desires the classifier to replace human decision making and an example should be considered adversarial if the classification task is easy for human observers but where the machine is wrong in unpredictable ways. In research on generation or mitigation of adversarial inputs, though, it has been difficult to perform perception in the loop: the underlying search technique exercises the network thousands of times, and it is impractical to ask the user at each step. Thus, most research has focused on using a metric on the input space, typically the  $L_0$ ,  $L_1$ ,  $L_2$ , or  $L_\infty$  norms, as a surrogate for human perception. Informally, for an image classification task, the  $L_0$  norm measures how many pixels differ, the  $L_1$  norm measures the sum of all pixel differences, the  $L_2$  norm the Euclidean distance, and the  $L_\infty$  norm the maximum difference in corresponding pixel values. Thus, algorithms to generate adversarial examples minimize the  $L_p$  norm between an original image and a new image that has a different classification and algorithms to mitigate against adversarial examples assume that a network is robust if it classifies close inputs in the  $L_p$  norm in the same way.

Unfortunately, this fundamental assumption may not hold. Several recent results have pointed out that these norms do *not* form reasonable measures of human perception of image similarity: inputs imperceptible to human observers may have high  $L_p$  norms, and vice versa [26]. This presents two technical obstacles to developing “human-level” classifiers. First, we know how to optimize for the wrong thing (an  $L_p$  norm) and we do not know how to scale the search with humans in the loop. Second, humans are better at providing *preferences* but not at providing quantitative norms. Thus, there is a problem of translating human perception of similarity into a norm usable by existing techniques.

In this paper, we present a method to find adversarial examples in DNNs in a *black box* setting that can directly use *human perception in the loop*. Black box means that we only have access to the input and the output of the network, but not to any other information such as the structure, the confidence levels at the output, or parameters of internal nodes. Perception in the loop means that our optimization procedure can explicitly ask human subjects their perceptual preferences in order to select inputs during the search.

We overcome the two technical difficulties in the following way. First, we base our search for adversarial examples on an *evolutionary search* technique. The specific search

strategy we use is *covariance matrix adaptation*-evolutionary strategy (CMA-ES) [13]. CMA-ES is a black box, gradient-free, search. It keeps a population of candidates, generated according to a distribution, and updates the distribution based on the “fittest” subset of candidates according to a fitness function. Specifically, in our context, CMA-ES works without any information about the structure of the network or confidence levels or gradients. In a first step, we show that CMA-ES with  $L_p$  norms can already outperform existing grey-box and black-box approaches (including those in [1], [23], [29]). Moreover, we empirically show that CMA-ES can find adversarial examples using small populations and few iterations: this sets the stage to include humans in the loop without high performance penalties.

Nominally, the top candidates in CMA-ES are chosen by ranking the candidates on the basis of a cost or “fitness” function, such as an  $L_p$  metric. Our insight is that CMA-ES does not, in fact, require a metric, but only an oracle to identify the “top  $K$ ” fittest individuals in the population. Thus, one could pick the top candidates based purely on perceptual preferences. In this way, our search is metric-free: in each phase, our CMA-ES search asks a human participant to pick the “top  $K$ ” inputs from the current population which are perceptually closest to a fixed, initial, input.

We show empirically that for standard benchmark sets (MNIST, CIFAR10, GTSRB), CMA-ES converges to an adversarial example with only a small population (at most 20) and in a small number of iterations (at most 200). Thus, it is feasible to ask a human participant a small number of questions (in our experiments, around 10) that already finds a misclassified example. We also demonstrate through a psychophysics experiment that perception of closeness among different human participants is robust to individual differences, and can be different from an  $L_p$  norm.

Altogether, we get a black-box adversarial input generator based directly on perceptual preferences. We compare the performance of CMA-ES against three main techniques: substitute training algorithm from [23], the GA algorithm from [1], and the MCTS algorithm from [29]. Our first set of experiments uses  $L_1$  and  $L_\infty$  norms and shows that black-box CMA-ES can be equal or more efficient in comparison with existing black- or grey-box techniques, both in the number of successes and in the average perturbation added. Next, we use CMA-ES to find adversarial examples on different datasets using human perception in the loop. Finally, we have also run our technique on networks that deliberately incorporate robustness in the training [19]. We show that while these networks are designed to be robust against  $L_\infty$  norm, we still find adversarial examples which are perceptually indistinguishable. Thus, we believe mitigation techniques should explicitly incorporate perceptual preferences as well.

We summarize our contributions.

- We use CMA-ES, an efficient black box optimization technique, to craft adversarial examples in a fully black box manner, without requiring knowledge about the network nor requiring training a new model.

- We propose the first perception-in-the-loop search for crafting adversarial examples and empirically demonstrate its efficiency on MNIST, CIFAR10, and GTSRB benchmarks.
- We demonstrate experimentally that perceptual preferences are robust across individuals.
- Using CMA-ES on robustly trained networks, we argue that networks should be made robust using human perception instead of other norms.

## II. RELATED WORK

*a) White-box adversarial examples:* Vulnerability of deep neural networks (DNNs) to adversarial inputs was pointed out in [3], [27]. Such adversarial examples were initially constructed by assuming full knowledge of the network’s architecture and its parameters. For example, [27] optimized the network’s prediction error and [11] used a fast gradient sign method to search for perturbed inputs with incorrect classification. The latter technique was extended in *DeepFool* [20] using variable gradient steps.

The papers [11] and [20] formulate the problem in a non-targeted manner, i.e., crafting adversarial examples for having an arbitrary misclassification (i.e., a classification different from the original input). Later, [24] proposed a *targeted* misclassification algorithm for finding perturbed inputs that result in a specific output classification. All these algorithms are *white box*: they use knowledge of the DNN architecture in the search for misclassifying perturbations.

*b) Black and grey-box adversarial examples:* In contrast to the *white-box* approaches, [23] proposed a *black-box* approach that does not require any knowledge of the network. Their approach requires access to the input-output data only but assumes accessibility of a fraction of the test data with which the DNN was evaluated. The approach of [23] has two stages for crafting adversarial examples. First, it feeds the DNN with significant amount of data, stores collected input-output pairs, and uses that data as labeled examples to train a substitute neural network with possibly different architecture. Once the substitute network is trained, they employ white-box methods such as the one in [11] to craft misclassifying examples, relying on a transference heuristic. The main disadvantage of this approach is that the adversarial examples are crafted on the substitute network, without any guarantee on misleading the original DNN. The implementation results of [23] also reveal that the transferability of the crafted adversarial samples is in general not very high.

Grey-box approaches craft adversarial inputs based on the input-output behavior as well as some extra information such as the output of the DNN’s softmax layer. For example, [29] craft adversarial examples in image classification tasks by first identifying the key points of the input image using object detection methods such as SIFT (Scale Invariant Feature Transform) and then using Monte Carlo tree search to select pixels around the key points which affect the softmax layer (the confidence levels) the most. In [21] another query-based local-search technique is proposed to choose pixels to perturb

which minimize confidence level associated with true class of the input image. [1] provides a gradient-free approach for crafting adversarial examples, based on Genetic Algorithms (GA). Later, [28] combines GA with a gradient-estimation technique to craft adversarial examples for applications in automatic speech recognition. [2], [5], use finite differences to estimate gradient of loss function which is then leveraged in white-box based attacks. In [16] a query-efficient method for estimating the gradient is proposed which is then leveraged to perform a projected gradient descent (PGD) update. However, their method requires several thousands of queries on average to mislead the DNN.

*c) Mitigation strategies:* The widespread existence of adversarial attacks led to research on mitigation strategies. The research can be divided into two categories: either improve the DNN robustness or detect adversarial examples. Strategies in the first category target at improving the training phase in order to increase the robustness and classification performance of the DNN. [11] suggests that adding adversarial samples to the training set can act as a regularizer. It is also observed in [23] that training the network with adversarial samples makes finding new adversarial samples harder. [10] shows that new samples can be obtained from a training set by solving a game between two DNNs. Recent papers [9], [19] have used *abstract interpretation* for training DNNs that are guaranteed to be robust. In particular, [19] constructs approximations of *adversarial polytopes*, which describe the set of possible neural network outputs given the region of possible inputs, and trains the network on the entire input space. This results in networks that are more robust. Most of this line of research pick a norm ( $L_1$  or  $L_\infty$ ) as a measure for robustness: the loss function during training ensures there is a neighborhood (in the chosen norm) around test inputs with the same classification. However, we show that our technique can find adversarial examples under the perceptual norm even on robustly trained networks.

The second category of strategies is reactive to the inputs and tries to identify adversarial samples by evaluating the regularity of samples [23]. These strategies are not effective against samples crafted by our approach: the optimization has human perception in the loop and crafts samples without irregularities seen in the outcome of other approaches.

*d) Choosing dissimilarity measures:* An adversarial example is found by adding perturbation to the original input image until the classifier is misled. Obviously, the classifier is not expected to classify the adversarial example the same as for the original input image if the amount of perturbation is high. An implicit assumption in most work on adversarial examples is that the inputs are *perceptually indistinguishable* to a human observer (see e.g., [4], [8], [25]). Most approaches for crafting adversarial examples have been founded on optimising a cost (or loss) function, typically  $L_p$  norms,  $p \in \{\infty, 0, 1, 2, \dots\}$ , as a proxy for human perception [11], [12], [23], [27]. For any two vectors  $v = [v_1, v_2, \dots, v_n]^T$  and  $v' = [v'_1, v'_2, \dots, v'_n]^T$  representing two images, their dissimilarity can be measured by  $L_0$  norm as  $\|v - v'\|_0 = \#\{i, v_i \neq v'_i\}$ , by  $L_\infty$  norm as

$\|v - v'\|_\infty = \max_i \{|v_i - v'_i|\}$ , or by  $L_p$  norm,  $p \in \{1, 2, \dots\}$ , as

$$\|v - v'\|_p = (\sum_{i=1}^n |v_i - v'_i|^p)^{\frac{1}{p}}.$$

In the context of adversarial examples,  $L_0$  measures the number of perturbed pixels,  $L_1$  gives the sum of absolute perturbations, and  $L_\infty$  measures the maximum perturbation applied to the pixels. The computation of  $L_p$  norm can be performed rapidly in computational tools; this is important because current techniques rely on a large number of evaluations of the dissimilarity measure. Thus, strategies for crafting adversarial examples and for mitigating them, rely on the assumption that the  $L_p$  norm evaluates dissimilarities close enough to the way humans interpret these differences.

Unfortunately, this assumption is not well-founded: inputs close in the  $L_p$  norms may be neither necessary nor sufficient for images to be perceptually similar [8], [17], [26]. Thus, a major open question is to incorporate perceptual measures directly in the training of machine learning classifiers.<sup>1</sup> The main challenges are that perceptual preferences do not directly provide a (differentiable) cost function, and involving a perceptual task in an exploration loop makes the search very slow.

We solve the problem of crafting adversarial inputs with perceptual similarity in the following way. First, our approach is black-box, and does not require finding gradients. Second, our approach using CMA-ES does not require a metric space on inputs, but only requires selecting the “top  $K$ ” closest inputs. Thus, we naturally incorporate an easy perception task (“pick the preferred  $K$  images”) in the search. We show empirically that the process converges in only a few iterations, making it feasible to find examples even with the cost of human perception in the loop. Finally, we show that the perceptual task is robust across humans and that top- $K$  perceptual selection performed by humans can be different from selecting the top  $K$  according to an  $L_1$  norm.

Use of perceptual preferences in learning and classification have been approached in other domains [6], [18], [30]. Our work demonstrates the applicability of perceptual preferences in the task of finding adversarial examples. We note that there is recent work on the “dual problem” of finding adversarial examples which fool both humans and machines [7]. Whether our approach generalizes to these problems or whether mitigation measures can use perception-in-the-loop is left for future work.

### III. THE ADVERSARIAL EXAMPLE PROBLEM

#### A. Deep Neural Networks

A classifier  $G : \mathbb{R}^d \rightarrow \{1, 2, \dots, L\}$  is a function that maps an input  $x \in \mathbb{R}^d$  to one of  $L$  possible labels. A deep neural network (DNN)  $\mathfrak{N}$  with *depth*  $n$  is a parameterised

<sup>1</sup> Of course, there are situations in which perceptual similarity is neither possible (e.g., in classification tasks unrelated to perception) nor the goal of an attack [22]; we focus on important scenarios where perception does play an important role.

representation of a classifier  $\mathcal{G}(\boldsymbol{\theta}, \cdot) : \mathbb{R}^d \rightarrow \mathbb{R}^L$  that is constructed by a forward combination of  $n$  functions:

$$\mathcal{G}(\boldsymbol{\theta}, x) := \mathcal{G}_n(\theta_n, \mathcal{G}_{n-1}(\theta_{n-1}, \dots \mathcal{G}_2(\theta_2, \mathcal{G}_1(\theta_1, x))))), \quad (1)$$

where  $x$  denotes the input to the DNN and  $\mathcal{G}_i(\theta_i, \cdot)$ ,  $i \in \{1, 2, \dots, n\}$ , denote non-linear functions (called *layers*), each parameterised by  $\theta_i$ . Each layer of the network  $\mathcal{G}_i$  takes its input as a representation of the input data and transforms it to another representation depending on the value of parameters  $\theta_i$ . The label associated to input  $x$  by the DNN  $\mathfrak{N}$  is obtained by finding the component of  $\mathcal{G}(\boldsymbol{\theta}, x)$  with the highest value:

$$\mathfrak{N}(\boldsymbol{\theta}, x) = \arg \max_{j \in \{1, 2, \dots, L\}} \mathcal{G}^{(j)}(\boldsymbol{\theta}, x), \quad (2)$$

where  $\mathcal{G}^{(j)}$  is the  $j$ th element of the output vector  $\mathcal{G}$ .

During the *training phase* of the network, the set of parameters  $\boldsymbol{\theta}$  is learnt using a large number of labeled input-output pairs  $\{(x_i, y_i) \mid i = 1, 2, \dots, m\}$  in order to achieve the highest performance by  $\mathfrak{N}(\boldsymbol{\theta}, \cdot)$  in mimicking the original unknown classifier  $G(\cdot)$  on the available data. During the *test phase* of the network,  $\mathfrak{N}$  is deployed with the fixed learned parameters  $\boldsymbol{\theta}_\ell$  and used to make predictions about the labels of inputs not seen during the training. The network is expected to generalize the training data set and to make accurate classifications on the test data set.

### B. Adversary's Goal

Given a network  $\mathfrak{N}$  with learned parameters  $\boldsymbol{\theta}_\ell$  and an input  $x$ , the goal of the adversary is to find an input  $x'$  such that  $\mathfrak{N}(\boldsymbol{\theta}_\ell, x') \neq \mathfrak{N}(\boldsymbol{\theta}_\ell, x)$ , i.e., the two images are classified in two different classes, while  $x, x'$  are “similar” as much as possible. One way to assess similarity is to define a metric space  $\|\cdot\|^*$  on the space  $\mathbb{R}^d$  of inputs, for example, using an  $L_p$  norm. Then, the *non-targeted* misclassification problem is to find

$$x_{\text{adv}}(x, \mathfrak{N}) = \arg \min_{x'} \{\|x - x'\|^*, \mid \mathfrak{N}(\boldsymbol{\theta}_\ell, x') \neq \mathfrak{N}(\boldsymbol{\theta}_\ell, x)\}. \quad (3)$$

The problem is *non-targeted* because we only require a misclassification and not any specific label for  $x_{\text{adv}}$ .

Alternatively, we can require a specific label for  $x_{\text{adv}}$ , and define the *targeted* misclassification problem:

$$x_{\text{adv}}(x, j, \mathfrak{N}) = \arg \min_{x'} \{\|x - x'\|^*, \mid \mathfrak{N}(\boldsymbol{\theta}_\ell, x') = j\},$$

for any  $j \neq \mathfrak{N}(\boldsymbol{\theta}_\ell, x)$ .

We present our results for non-targeted misclassification but the results are applicable to the targeted case as well. In the experimental results of Section V, we use  $L_1$  and  $L_\infty$  norms for measuring distances between inputs in order to compare our results with the approaches in the literature.

For perception in the loop, we use the following formulation:

$$x_{\text{adv}}(x, \mathfrak{N}) = \arg \min_{x'} \{d_{\text{per}}(x, x'), \mid \mathfrak{N}(\boldsymbol{\theta}_\ell, x') \neq \mathfrak{N}(\boldsymbol{\theta}_\ell, x)\}, \quad (4)$$

where we require that the function  $d_{\text{per}}(x, x')$  is such that for any fixed  $x$ ,  $d_{\text{per}}(x, \cdot)$  induces a total order on the set of inputs.

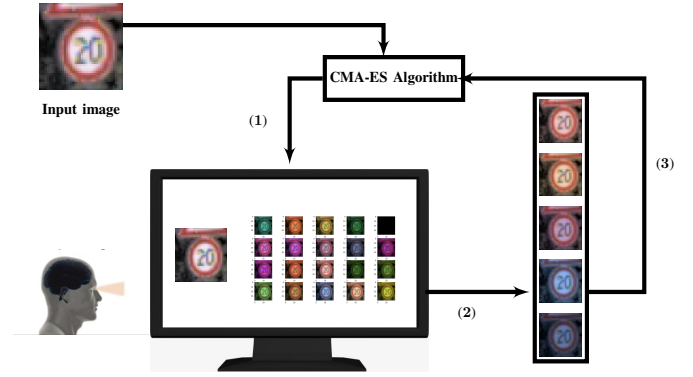


Fig. 1. Running CMA-ES with human in the loop that includes (1) generating certain number of adversarial candidates by the CMA-ES; (2) selecting top candidates most similar to the reference image by the user; (3) feeding selected candidates back to the CMA-ES.

Formally,  $d_{\text{per}}(x, \cdot)$  is antisymmetric and transitive, and for any  $x', x''$ , either  $d_{\text{per}}(x, x') \leq d_{\text{per}}(x, x'')$  or  $d_{\text{per}}(x, x'') \leq d_{\text{per}}(x, x')$ . With these properties, we can solicit preferences from human users to select the top  $k$  inputs from a set which are “most similar” to a given input.

### C. Adversary's Capabilities

We work in the black-box setting. The adversary can query the DNN  $\mathfrak{N}$  on a given input  $x$  and receive the output label  $\mathfrak{N}(\boldsymbol{\theta}_\ell, x)$ . However, the adversary does not know the depth, the parameters  $\boldsymbol{\theta}_\ell$ , or the confidence levels. This assumption makes adversaries considered in our work weaker but more realistic in comparison with the ones in [11], [27], [29], since output labels contain less information about the model's behavior. Note that gradient based methods of [11], [24], [27] cannot be utilized for crafting adversarial examples since the adversary has no knowledge of the DNN's parameters or confidence levels.

## IV. COVARIANCE MATRIX ADAPTATION EVOLUTION STRATEGY (CMA-ES)

### A. Basic Algorithm

CMA-ES [13] is an efficient optimization method belonging to the class of evolutionary algorithms. It is stochastic and derivative-free, and can handle non-linear, non-convex, or discontinuous optimization problems. It is based on the principle of biological evolution that is inspired by the repeated interplay of variation and selection.

The algorithm proceeds in generations. In each generation, it generates a new population of candidate solutions by *variation* of the “best” candidates of the previous generation in a stochastic way. Then, it ranks a subset of the current population according to a fitness function; this subset becomes the parents in the next generation. This leads to get more and more individuals with better fitness over successive generations. CMA-ES has been shown to be very efficient on a number of domains [14], [15], without requiring large sample populations or carefully scaled fitness functions [13].

New individuals are sampled from a multivariate normal distribution whose parameters are updated using the parents from the previous generation. Variation is captured by updating the mean value of the distribution and adding a zero-mean stochastic perturbation. CMA-ES adapts the covariance matrix of the distribution by learning a second order model of the underlying fitness function. CMA-ES requires only the ranking between candidate solutions in order to learn the sample distribution: neither derivatives nor the function values are needed.

We present the essential steps of the CMA-ES algorithm following [13]. Let us fix the size of the population  $L \geq 2$  for each generation and a parameter  $K < L$ . The parameter  $K$  determines the size of the ‘‘most fit’’ sub-population that will be used to update the distribution in the next generation. In each generation  $g = 0, 1, \dots$ , the algorithm maintains an  $n$ -dimensional multivariate normal distribution  $(\mu^g, C^g, \gamma^g)$  with mean  $\mu^g$ , covariance matrix  $C^g$ , and step size  $\gamma^g$ . Here,  $n$  is the dimension of the solution.

To go from generation  $g$  to generation  $g+1$ , we first sample a population of  $L$  new individuals using the multivariate distribution from the previous generation:

$$x_i^{(g+1)} = \mu^{(g)} + \gamma^{(g)} z_i^{(g+1)}, \quad z_i^{(g+1)} \sim \mathcal{N}(0, C^{(g)}), \quad (5)$$

for  $i = 1, \dots, L$ . Based on this population, we update the parameters  $(\mu, C, \gamma)$  of the distribution for the  $(g+1)$ st generation.

The individuals  $x_i^{(g+1)}$ ,  $i \in \{1, \dots, L\}$  are first ranked according to some fitness function. Let  $\{i_1, \dots, i_L\}$  be a permutation of  $\{1, \dots, L\}$  such that  $x_{i_1}^{(g+1)}, x_{i_2}^{(g+1)}, \dots, x_{i_L}^{(g+1)}$  is a ranked version of the individuals in the  $(g+1)$ st generation from the best to the worst fitness.

Then the mean value is updated according to

$$\mu^{(g+1)} = \mu^{(g)} + c_m \sum_{s=1}^K \omega_s \left[ x_{i_s}^{(g+1)} - \mu^{(g)} \right], \quad (6)$$

where  $c_m \leq 1$  is the learning rate, usually set to 1, and  $\omega = [\omega_1, \omega_2, \dots, \omega_L]$  is a weight vector with the property that  $\sum_{s=1}^K \omega_s = 1$ ,  $\omega_1 \geq \omega_2 \geq \dots \geq \omega_K > 0$ , and  $\omega_s \leq 0$  for  $s > K$ .

The covariance matrix is updated as follows:

$$C^{(g+1)} = \left[ 1 - c_1 - c_2 \sum_{i=1}^L \omega_i \right] C^{(g)} + c_1 P_c^{(g+1)} P_c^{(g+1)T} + c_2 \sum_{i=1}^L \omega_i z_i^{(g+1)} z_i^{(g+1)T}, \quad (7)$$

where  $c_1$  and  $c_2$  are learning rates corresponding to the rank one and the rank  $K$  covariance updates. The vector  $P_c^{(g)} \in \mathbb{R}^n$  denotes the *evolution path* in the  $g$ th generation and is updated according to the following adaptation law:

$$P_c^{(g+1)} = (1 - c_3) P_c^{(g)} + \sqrt{c_3(2 - c_3)\kappa} \frac{\mu^{(g+1)} - \mu^{(g)}}{\gamma^{(g)}}, \quad (8)$$

where,  $c_3 \leq 1$  is a learning rate for path evolution update and  $\kappa := 1/\sum_{s=1}^K \omega_s^2$ .

Finally, the step size is updated as follows:

$$\gamma^{(g+1)} = \gamma^{(g)} \exp \left[ \frac{c_\gamma}{d_\gamma} \left( \frac{\|P_\gamma^{(g+1)}\|}{E} - 1 \right) \right], \quad (9)$$

where  $c_\gamma < 1$  and  $d_\gamma$  denote respectively the learning rate and damping factor for the step size update. We define the constant  $E := \sqrt{2\Gamma(\frac{n+1}{2})}/\Gamma(\frac{n}{2})$ , where  $\Gamma$  is the gamma function. Finally,  $P_\gamma^{(g)}$  is the *conjugate evolution path* with the adaptation law

$$P_\gamma^{(g+1)} = (1 - c_\gamma) P_\gamma^{(g)} + \sqrt{c_\gamma(2 - c_\gamma)\kappa} \left[ C^{(g)} \right]^{-\frac{1}{2}} \frac{\mu^{(g+1)} - \mu^{(g)}}{\gamma^{(g)}}, \quad (10)$$

where  $C^{(g)-\frac{1}{2}}$  is the square root of the covariance matrix defined as  $C^{(g)-\frac{1}{2}} := BD^{-1}B^T$  with  $C^{(g)} = BD^2B^T$  being an eigen-decomposition of  $C^{(g)}$ .

We emphasize that the updates to the parameters *only depend on the top  $K$  individuals and not on their relative order*. While a linear ranking function is one way to determine the top  $K$  individuals, the CMA-ES algorithm only requires determining the top  $K$  individuals in each generation.

## B. Fitness Functions

We now provide fitness functions in our setting.

Suppose a DNN  $\mathfrak{N}(\theta_\ell, \cdot)$  and a reference input  $x_{\text{ref}}$  are given. When using  $L_p$  norm, we rank the randomly generated inputs in the CMA-ES algorithm using the fitness function

$$f(x) := \begin{cases} \|x - x_{\text{ref}}\|_p & \text{if } \mathfrak{N}(\theta_\ell, x) \neq \mathfrak{N}(\theta_\ell, x_{\text{ref}}) \\ M_1 + M_2 \|x - x_{\text{ref}}\|_p & \text{if } \mathfrak{N}(\theta_\ell, x) = \mathfrak{N}(\theta_\ell, x_{\text{ref}}), \end{cases} \quad (11)$$

where  $M_1, M_2 > 1$  are very large constants. Then  $x_i^{(g+1)}$ ,  $i = 1, 2, \dots, L$  are ranked such that

$$f(x_{i_1}^{(g+1)}) \leq f(x_{i_2}^{(g+1)}) \leq \dots \leq f(x_{i_L}^{(g+1)}).$$

Note that  $f(\cdot)$  assigns very large values to inputs within the same class as  $x_{\text{ref}}$  and reduces the chance of having them as parents for the next generation. Note that the fitness function (11) is not continuous.

When using human perception, the algorithm generates a population of new inputs and filters any image in the same class as the original input  $x_{\text{ref}}$ . The filtered sub-population is displayed to the user, who is asked to pick the top  $K$  inputs from the sub-population perceptually similar to  $x_{\text{ref}}$ . Fig. 1 shows a schematic of our implementation.

## C. Improving Performance of CMA-ES Using Bisection

To find adversarial inputs, we augment the basic CMA-ES search using a bisection technique. Briefly, we run CMA-ES for a number of iterations to find a misclassified input and then search for another misclassified input closer to the original input by iteratively reducing certain dimensions and checking if the resulting input is still misclassified.

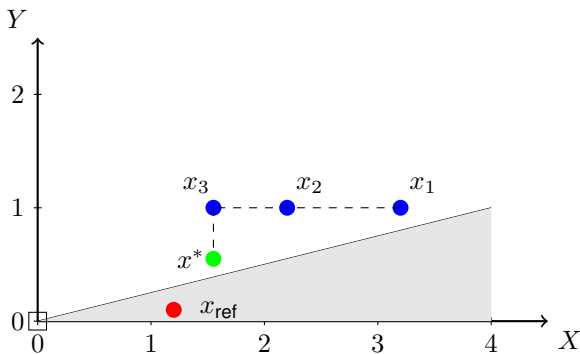


Fig. 2. Graphical demonstration for bisection method;  $x_{\text{ref}}$  is the two-dimensional input;  $x_1$  is the example generated by CMA-ES after a few iterations;  $x_2$ ,  $x_3$  and  $x^*$  are computed by running bisection.

Fig. 2 summarizes the technique when there are two labels, grey and white, separated by a linear boundary. Suppose we start from an input  $x_{\text{ref}}$  (shown as a red dot) and run CMA-ES to get a misclassified example  $x_1$ . Then, we consider the dimension  $i$  of  $x_1$  for which  $|x_1^i - x_{\text{ref}}^i|$  is the largest. We consider a new input which replaces the  $i^{\text{th}}$  coordinate of  $x_1$  by  $(x_1^i + x_{\text{ref}}^i)/2$ . In our example, this new point  $x_2$  is still misclassified, and we repeat the process with  $x_2$  and  $x_{\text{ref}}$ , getting subsequently a new point  $x_3$ , and so on. In case the new point was not misclassified, we increase the  $i^{\text{th}}$  coordinate and continue exploring the same dimension. We continue in this way to find a new misclassified input  $x^*$  closer to  $x_{\text{ref}}$  for a pre-specified number of steps. In our experiments, this bisection technique significantly reduced the distance between the original input and the misclassified input when  $L_\infty$  is used for assessing similarities between images.

## V. EXPERIMENTAL RESULTS: $L_p$ NORMS

We have implemented the CMA-ES algorithm to find adversarial examples. Our experiments had the following aims.

**Baseline Performance** Compare the performance of CMA-ES when using  $L_1$  and  $L_\infty$  norms with other grey- and black-box techniques in the literature.

**Perception-in-the-Loop** Find adversarial examples using human perception in the loop. As part of this process, we also evaluate the robustness of perceptual preferences.

In this section, we report results of using CMA-ES in crafting adversarial examples using  $L_1$  and  $L_\infty$  norms, and compare its performance with existing algorithms. The aim of this comparison is to show that black-box CMA-ES is comparable in efficiency to existing black- or grey-box techniques and to establish a baseline performance that is used to determine population size and number of iterations for perception-in-the-loop experiments. In Section VI, we report on running CMA-ES using perception in the loop.

We have conducted experiments on three popular image recognition benchmarks: MNIST, GTSRB, and CIFAR10. We compare the performance of CMA-ES against three main techniques: substitute training algorithm from [23], the GA

algorithm from [1], and the MCTS algorithm from [29]. Recall that the first two are black-box approaches while the third is grey box. We use  $L_1$  norm in the fitness function of all these algorithms with a fixed number of queries. Given two images  $x$  and  $x'$  with  $k$  channels and resolution  $h \times w$ , the *average perturbation* in the  $L_1$  norm sense is defined as:

$$d(x, x') = \frac{\|x - x'\|_1}{k \times h \times w}. \quad (12)$$

### A. Benchmarking CMA-ES on MNIST

The MNIST dataset is considered to be the most common benchmark in many previous studies for crafting adversarial examples. It consists of 60000 grey scale images of handwritten digits, with resolution  $28 \times 28$  for training, as well as 10000 images for testing. We split the training dataset into training (80%) and validation (20%) sets. We trained two DNNs proposed for MNIST, labeled DNN A ([23]) and DNN B<sup>2</sup> in Table I. The DNNs are of type LeNet and consist of input, convolutional, max pooling, fully connected, and softmax layers. Both DNNs are trained for 10 epochs with learning rate of 0.001 and the achieved accuracies for DNN A and DNN B on the 10000 test images are 98.36% and 97.73% respectively, which is close to the accuracy of state-of-the-art classifiers on MNIST [29].

We conducted our experiments in the following way. For each class, we generated 10 randomly selected images from test dataset, which are classified correctly by the DNN. For each image, first, CMA-ES was run for 180 iterations, with population size 4 ( $L = 4$ ) and parent size 2 ( $K = 2$ ). This took about 15 seconds in average. In order to compare our result with the black-box algorithm proposed in [23], we used their own implementation for MNIST dataset: 150 samples from test data were used in input data augmentation; for training of substitute network, the DNN's output label was read 6400 times; the architecture of the substitute NN includes input and output layers as well as two fully connected layers with 200 neurons each.

For the genetic algorithm based crafting method [1], we achieved the best performance by running GA for 120 generations including 6 individuals, and setting the mutation rate to be 0.05, as given in [1]. For GA implementation, we used the same fitness function as CMA-ES. Notice that the query length in both GA and CMA-ES is set to 720.

Finally, we took one of the most powerful grey-box adversarial example crafting methods, proposed in [29] into account. Their algorithm is based on Monte Carlo Tree Search (MCTS). Apart from GA, for the rest of methods, we ran authors' provided codes for both DNN A and B setting all the parameters to their default values. Tables II and III list results of running all four methods mentioned above. For GA and CMA-ES, the success rate is 100%, meaning that for 100% of tested inputs, an adversarial example is found. However, success rate for substitute training and MCTS methods is 89%.

<sup>2</sup>Using available code at <https://mathworks.com>

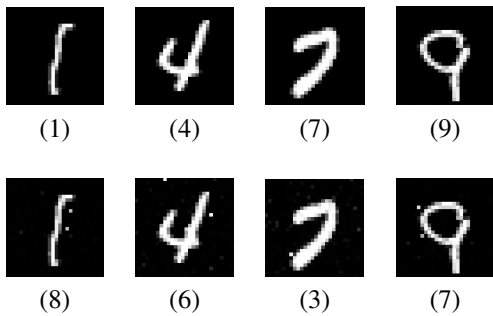


Fig. 3. Top: Original samples from MNIST dataset; Bottom: Misclassified examples generated by CMA-ES for inputs from top row

We measure the performance in terms of average perturbation, using (12). It can be noticed that apart from MCTS, CMA-ES’s performance is significantly better, but the performance of CMA-ES and MCTS is close. However, CMA-ES is superior in terms of success rate.

In all experiments, CMA-ES always found adversarial examples with less than 7% perturbation in the  $L_1$  norm sense. As a concrete example, Fig. 3 illustrates the case for which the four input images shown on the top row are classified by the DNN correctly; however, CMA-ES is able to find within 15s the corresponding perturbed images, shown on the bottom row, which are misclassified by the DNN. Increasing the number of iterations for CMA-ES while fixing other parameters results in even smaller perturbations.

### B. Benchmarking CMA-ES on GTSRB

The German Traffic Sign Recognition Benchmark (GTSRB) includes colored (3-channel) images with different sizes. After resizing and removing the frames of images, the GTSRB dataset contains 39209 3-channel  $40 \times 40$  pixel images for training, as well as 12600 test images. We split the training set into training (80%) and validation (20%) sets. We used a previously proposed convolutional neural network (DNN E in Table I)<sup>3</sup> of type LeNet and consisting of input, convolution ( $\times 6$ ), max pooling ( $\times 3$ ), fully connected ( $\times 1$ ), softmax, and output layers. The DNN is trained for 32 epochs with learning rate of 0.0001. The achieved accuracy of the trained DNN on 12600 test data is 96.53%.

In order to generate adversarial examples, first, we took all the 1600 pixels into consideration as optimization variables for CMA-ES. Again, for each of the classes, we chose 10 random samples from test dataset and ran CMA-ES to find 1600 values as elements of the perturbation vector. We set the number of iterations to 180, population size to 4 ( $L = 4$ ) and parent size to 2 ( $K = 2$ ). The overall success rate was 97.3% and average perturbation rate was 4.19%. Some of the misleading examples crafted by CMA-ES are demonstrated in Fig. 4.

<sup>3</sup>Using available code at <https://chsasank.github.io/keras-tutorial.html>



Fig. 5. Original image labeled by DNN as "STOP" (Left) and perturbed image classified as "No entry" after adding 4% noise (Right)

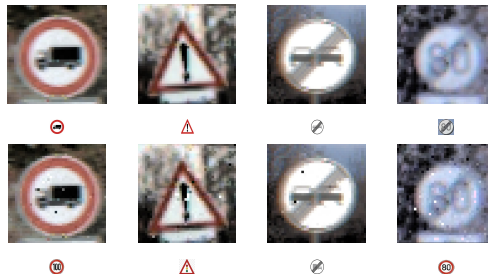


Fig. 4. Top: Original examples from GTSRB dataset; Bottom: Misclassified examples generated by CMA-ES for inputs from top row using pixel perturbation

We noticed, as in [26], that for RGB photos, there were cases in which small perturbations in the pixel level (in  $L_1$  norm sense) was not compatible with human perception. One such example is shown in Fig. 5 in which adding 4.01% perturbation makes the image fuzzy. Thus, in a second experiment, we changed the perturbation criterion to three values  $\beta_r, \beta_g, \beta_b$  as darkening factors for red, green and blue channels respectively. These darkening factors are in the interval  $[0, 1]$ , being equal to one means no perturbation and being equal to zero means fully darkened. For this new setting, the objective function Eq. (11) can be written as

$$f(x) := \begin{cases} 3 - (\beta_r + \beta_g + \beta_b) & \text{if } \mathfrak{N}(\theta_\ell, x) \neq \mathfrak{N}(\theta_\ell, x_{\text{ref}}) \\ M & \text{if } \mathfrak{N}(\theta_\ell, x) = \mathfrak{N}(\theta_\ell, x_{\text{ref}}), \end{cases} \quad (13)$$

where  $M > 3$  is a large number. The number of iterations was set to 3, population size was 240, and parent size was 120. Running CMA-ES in this setting results in 100% success rate. Fig. 6 demonstrates some examples of adversarial images crafted by changing color combinations.

### C. Benchmarking CMA-ES on CIFAR10

The CIFAR10 dataset contains 60000  $32 \times 32$  color images (three channels) in 10 classes, with 6000 images per class. There are 50000 training images and 10000 test images. We trained a previously proposed convolutional neural network (DNN D in Table I)<sup>4</sup> with convolution ( $\times 2$ ), max pooling ( $\times 2$ ), fully connected ( $\times 1$ ), and softmax layers, which achieved 72.3% test accuracy.

In order to generate adversarial examples, we considered pixel perturbations with all 1024 pixels as optimization vari-

<sup>4</sup>Using available code at <https://chsasank.github.io/keras-tutorial>

TABLE I

DESCRIPTION OF THE DNN ARCHITECTURES USED IN THIS PAPER. ID: REFERENCE MENTIONED IN THE PAPER; INPUT: INPUT DIMENSION; CONV( $a \times b$ ): CONVOLUTIONAL LAYER WITH  $a \times b$  KERNELS FOLLOWED BY MAX-POOLING WITH  $2 \times 2$  KERNEL AND RELU AS ACTIVATION FUNCTION; FC: FULLY CONNECTED LAYER; S: SOFTMAX LAYER.

ID	Input	Conv	Conv	Conv	Conv	Conv	Conv	Conv	FC	S
A	784	32 ( $2 \times 2$ )	64 ( $2 \times 2$ )	-	-	-	-	-	-	10
B	784	20 ( $5 \times 5$ )	-	-	-	-	-	-	-	10
C	784	16 ( $4 \times 4$ )	32 ( $4 \times 4$ )	-	-	-	-	-	100	10
D	3072	32 ( $3 \times 3$ )	32 ( $3 \times 3$ )	64 ( $3 \times 3$ )	64 ( $3 \times 3$ )	-	-	-	512	10
E	4800	32 ( $3 \times 3$ )	32 ( $3 \times 3$ )	64 ( $3 \times 3$ )	64 ( $3 \times 3$ )	128 ( $3 \times 3$ )	128 ( $3 \times 3$ )	128 ( $3 \times 3$ )	512	43

TABLE II

COMPARING CMA-ES WITH OTHER BLACKBOX METHODS FOR CRAFTING ADVERSARIAL EXAMPLES ON MNIST DATA (DNN A)

Method	0	1	2	3	4	5	6	7	8	9
CMA-ES	1.80%	0.91%	2.99%	3.66%	3.96%	6.59%	4.51%	2.30%	3.51%	1.04%
Substitute Training [23]	32%	38.33%	57%	47.5%	42.66%	67.33%	41.33%	39.66%	40.37%	37.33%
GA	15.69%	12.81%	18.52%	19.22%	18.05%	19.14%	18.8%	15.56%	16.31%	15.12%
MCTS [29]	2.44%	2.18%	1.97%	2.09%	2.1%	1.96%	2.81%	2.11%	2.45%	1.73%

TABLE III

COMPARING CMA-ES WITH OTHER BLACKBOX METHODS FOR CRAFTING ADVERSARIAL EXAMPLES ON MNIST DATA (DNN B)

Method	0	1	2	3	4	5	6	7	8	9
CMA-ES	0.75%	0.93%	0.33%	1.36%	1.94%	2.27%	3.9%	0.9%	2.9%	0.72%
Substitute Training [23]	22%	25.18%	51.33%	37.61%	27.66%	37.03%	45.71%	23.33%	37.66%	38%
GA	10.07%	10.28%	15.23%	14.27%	11.92%	14.55%	14.29%	9.81%	11.18%	10.79%
MCTS [29]	1.54%	1.61%	1.95%	2.11%	1.98%	1.88%	1.89%	1.72%	1.81%	1.61%

TABLE IV

CRAFTING ADVERSARIAL EXAMPLES ON CIFAR10 DATA USING CMA-ES

Source class	plane	car	bird	cat	deer	dog	frog	horse	ship	truck
Mean pert	0.67%	0.83%	0.38%	0.49%	0.51%	0.50%	3.98%	0.71%	0.90%	1.38%
Success rate	100%	100%	100%	100%	100%	100%	100%	100%	100%	100%

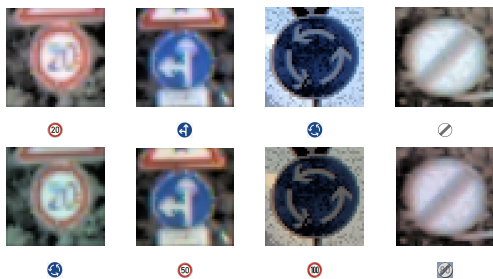


Fig. 6. Top: Original examples from GTSRB dataset; Bottom: Misclassified examples generated by CMA-ES for inputs from top row using color combination change

ables of CMA-ES. The number of iterations was 180, population size was  $L = 4$ , and parent size was  $K = 2$ . For each of the classes, we chose 10 random samples from the test dataset and generated the adversarial examples. Fig. 7 demonstrates four of these examples. Table IV shows the average perturbation and the corresponding success rate for each of the classes. The overall success rate is 100% with

average perturbation 1.02%.

As with GTSRB, we ran CMA-ES with perturbations  $\beta_r, \beta_g, \beta_b$  on darkening colors. We ran CMA-ES for 3 iterations, with a population size of  $L = 240$  and parent size of  $K = 120$ . Fig. 8 shows four of the original and the corresponding adversarial examples. The success rate was again 100% with average perturbation 17%.



Fig. 8. Top: Original examples from CIFAR10 dataset; Bottom: Misclassified examples generated by CMA-ES for inputs from top row using color combination change

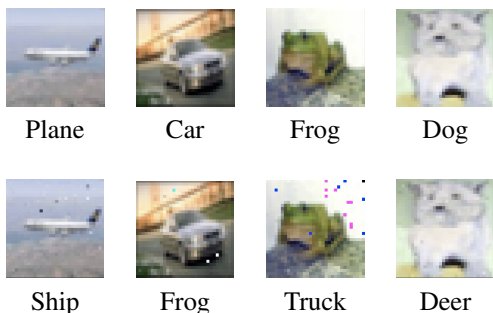


Fig. 7. Top: Original examples from CIFAR10 dataset; Bottom: Misclassified examples generated by CMA-ES for inputs from top row using pixel perturbation

#### D. Benchmarking CMA-ES using $L_\infty$ norm

In this section, we briefly discuss the results on using  $L_\infty$  norm in the fitness function. We ran CMA-ES on the MNIST dataset using  $L_\infty$  norm. In this experiment, we randomly selected 10 input images from each class of MNIST and set iteration number, population number ( $L$ ) and parent number ( $K$ ) to 3, 240 and 120 respectively. Table V shows the average perturbations in the  $L_\infty$  sense to find misclassified examples with and without bisection. One can notice that bisection significantly improves the performance of CMA-ES in this experiment, although the perturbations were relatively larger than all the cases when  $L_1$  are used.

Overall, our experiments indicate that one can find adversarial examples using CMA-ES on a wide class of image recognition benchmarks with a small number of iterations, and small population sizes.

## VI. EXPERIMENTS WITH PERCEPTION IN THE LOOP

In this section, we describe our experiments running CMA-ES with human perception as the fitness function. We describe three experiments. The first experiment (Section VI-A) is a human subject experiment to check that perceptual preferences is robust to individual participants. This is important to ensure our subsequent study is not biased by the specific user. The second experiment runs CMA-ES to find adversarial examples. Finally, the third experiment shows that a DNN trained to be robust against  $L_\infty$  norm can nevertheless misclassify examples when run with perception-in-the-loop.

### A. Comparing human perception with $L_1$ norm

In this experiment, we study the robustness of perceptual similarity across human subjects. Twenty students and researchers (15 male, 5 female; age range 22-36 years) participated in this experiment. The observers were naïve to the purpose and the nature of the experiment. All participants had normal or corrected-to-normal vision. They volunteered to participate in the experiment and gave informed consent in accordance to the policies of our university’s Committee for the Protection of Human Subjects, which approved the experimental protocol.

Each stimulus in the experiment consisted of a single image (the source) and upto 20 related images. The participants were

shown the set of images simultaneously and had to pick the 5 images closest to the source.

In order to create the stimuli, we selected 10 sample images out of test dataset for GTSRB and CIGFAR10. For each image, we run perception based CMA-ES for 3 iterations, setting  $L = 20$  and  $K = 5$ . After 3 iterations, we stopped CMA-ES and stored the population at the last iteration. Finally, only misclassifying examples were kept. Since  $L = 20$ , this number could be 20 at maximum.

Suppose that  $i^{th}$  participant selects 5 indexes for the  $j^{th}$  image. Then, we define  $h_{ij}$  as a  $20 \times 1$  binary vector with 1s at places corresponding to the selected indexes and 0s elsewhere. Doing so, we can compute mean vector  $\bar{h}_i$  for the  $i^{th}$  image. Therefore, we can measure spread of choices, using the following relation:

$$\epsilon = \frac{1}{(n_p \times n_e)} \sum_{j=1}^{n_e} \sum_{i=1}^{n_p} \frac{\|h_{ij} - \bar{h}_i\|_1}{2}$$

In above relation,  $n_p$  and  $n_e$  denote number of participants and examples, respectively. In our case,  $n_p = 20$  and  $n_e = 10$ . Furthermore, division by 2 is included since  $h_{ij}$ s are complementary for elements at which they are different. In our case,  $\epsilon = 0.7327$ . Intuitively, this means that participants are different in less than one choice in average.

We also computed  $H_j$  similar to  $h_{ij}$ , but with respect to  $L_1$  norm ranking. Again, we define

$$E = \frac{1}{n_e} \sum_{j=1}^{n_e} \frac{\|H_j - \bar{h}_j\|_1}{2}$$

to measure difference between the  $L_1$  norm selection and average of participants. We computed  $E = 1.1844$ . Intuitively, this means that participants’ ranking (in average) is different from what  $L_1$  norm suggests in more than one choice.

These results show that human perception is robust across participants and moreover, the  $L_1$  norm based ranking is different compared to a ranking based on human perception.

### B. CMA-ES with Perception-in-the-Loop

We now present adversarial input generation using CMA-ES with human perception. The goal is to come up with more realistic adversarial examples with respect to human’s judgment. In order to achieve this goal we do the following. First, CMA-ES is used to generate a population of inputs. The original input and the entire population is displayed together on a screen. However, any input classified the same way as the original input is hidden and displayed as a fully black square. The user looks at the original image and the current set of adversarial examples. By comparing each example with the original image, the user selects the top  $K$  examples closest to the original input. We do not restrict the time of the user to make a decision.

This process is demonstrated schematically in Fig. 1. For example in Fig. 9, the top image shows a traffic sign and the next images show 3 iterations of running CMA-ES. In this example, the population size was set to 20 and the user had

TABLE V  
COMPARING PERFORMANCE OF CMA-ES USING  $L_\infty$  NORM WITH AND WITHOUT BISECTION

Source class	0	1	2	3	4	5	6	7	8	9
Using bisection	17.95%	22.16%	20.82%	15.1%	28.63%	13.89%	36.68%	21.4%	20.92%	26.31%
Pure CMA-ES	52.36%	58.69%	63.63%	60.04%	51.01%	62.03%	66.33%	60.48%	58.21%	51.86%

to pick the top 5 closest images. Given the choice, CMA-ES updates its parameters and generates second set of examples. This process continues until the last iteration in which user selects the best example.

Fig. 11 demonstrates three sample outputs of running CMA-ES using human perception, where the number of iterations was 180, population size was 4, and parent size was 2. Thus, the user had to solve 180 perception tasks.

Next, we evaluate CMA-ES with perception-in-the-loop when the number of iterations is reduced, in order to reduce the burden on the user. We consider CMA-ES with only 100 iterations, with a population size of 4 and parent size of 2. Fig. 12 demonstrates two examples in which images from GTSRB and corresponding adversarial samples crafted using  $L_1$  norm and human perception, with pixel perturbations. Subjectively, the human perception version looks “better.”

The effects are even more marked when using color recombinations. Fig. 13 demonstrates several examples from GTSRB and CIFAR10 datasets as well as corresponding misclassifying image using  $L_1$  and human perception, when the number of iterations was 3 and the population size and parent size were 20 and 5, respectively. Subjectively, the color schemes for perception-in-the-loop was closer to the original image.

### C. Attacking Robustly Trained DNNs

Finally, we consider adversarial input generation for DNNs which are trained to be robust against perturbations. We consider robust training based on abstract interpretation [19], which encodes  $\epsilon$ -robustness in  $L_\infty$  norm into the loss function, for a user-defined parameter  $\epsilon$ . The goal is to ensure that each training input has an  $\epsilon$ -neighborhood with the same classification.

We trained a DNN from [19] for the MNIST dataset. It has convolutional layers ( $\times 2$ ), maxpooling layers ( $\times 2$ ), and fully connected layer before the softmax layer (DNN C in Table I [19]). We trained this network using their “box” method and with 4 different perturbation parameters ( $\epsilon$ ). After training for 180 epochs, we evaluated the robustness of the network against two attacks: fast gradient sign method (FGSM) with the same  $\epsilon$  used in training and CMA-ES with perception in the loop.

We ran CMA-ES for 3 iterations, with population size 240 and parent size 120. CMA-ES was agnostic to the  $\epsilon$  parameter, and considered those generated examples which could be classified by human eyes correctly, as adversarial examples. Table VI summarizes the results. While FGSM had a low success rate, CMA-ES was able to synthesize perceptually similar adversarial examples, albeit with a lower success rate than DNN A or B with standard training.

TABLE VI  
COMPARISON BETWEEN SUCCESS RATES OF FGSM (BASED ON  $L_\infty$ ) AND CMA-ES (BASED ON PERCEPTUAL NORM)

$\epsilon$	0.02	0.05	0.1	0.15	0.2
FGSM	0%	0%	10%	23.3%	36.7%
CMA-ES	46.7%	46.7%	73.3%	76.7%	83.3%

An implication of this experiment is that while for some  $\epsilon$ , the network is quite robust with respect to  $L_\infty$  norm, it is still prone to attacks which are based on perceptual norm. Intuitively, this means that the measuring robustness of trained NNs solely using  $L_p$  norms is not sufficient. Fig. 14 demonstrates some examples crafted by CMA-ES in 180<sup>th</sup> epoch.



Fig. 14. Some examples of misclassified images crafted on robustly trained CNN with [19]

## VII. CONCLUSION

We have presented a technique to construct adversarial examples based on CMA-ES, an efficient black box optimization technique. Our technique is black box and can directly use human perceptual preferences. We empirically demonstrate that CMA-ES can efficiently find perceptually similar adversarial inputs on several widely-used benchmarks. Additionally, we demonstrate that one can generate adversarial examples which are perceptually similar, even when the underlying network is trained to be robust using  $L_p$  norm. While we focus on incorporating perceptual preferences in crafting adversarial inputs, the role of direct perceptual preferences in mitigating against attacks is left for future work.

## REFERENCES

- [1] Moustafa Alzantot, Yash Sharma, Supriyo Chakraborty, and Mani B. Srivastava. GenAttack: Practical black-box attacks with gradient-free optimization. *CoRR*, abs/1805.11090, 2018.
- [2] Arjun Nitin Bhagoji, Warren He, Bo Li, and Dawn Song. Exploring the space of black-box attacks on deep neural networks. *CoRR*, abs/1712.09491, 2017.
- [3] B. Biggio, I. Corona, D. Maiorca, B. Nelson, N. Srndić, P. Laskov, G. Giacinto, and F. Roli. Evasion attacks against machine learning at test time. In *ECML PKDD*. ACM, 2013.
- [4] Nicholas Carlini and David A. Wagner. Towards evaluating the robustness of neural networks. In *2017 IEEE Symposium on Security and Privacy, SP 2017, San Jose, CA, USA, May 22-26, 2017*, pages 39–57, 2017.

- [5] Pin-Yu Chen, Huan Zhang, Yash Sharma, Jinfeng Yi, and Cho-Jui Hsieh. ZOO: Zeroth order optimization based black-box attacks to deep neural networks without training substitute models. In *Proceedings of the 10th ACM Workshop on Artificial Intelligence and Security, AISec '17*, pages 15–26, New York, NY, USA, 2017. ACM.
- [6] Paul F. Christiano, Jan Leike, Tom B. Brown, Miljan Martic, Shane Legg, and Dario Amodei. Deep reinforcement learning from human preferences. In *Advances in Neural Information Processing Systems 30: Annual Conference on Neural Information Processing Systems 2017, 4-9 December 2017, Long Beach, CA, USA*, pages 4302–4310, 2017.
- [7] Gamaleldin F. Elsayed, Shreya Shankar, Brian Cheung, Nicolas Papernot, Alex Kurakin, Ian J. Goodfellow, and Jascha Sohl-Dickstein. Adversarial examples that fool both human and computer vision. *CoRR*, abs/1802.08195, 2018.
- [8] Logan Engstrom, Dimitris Tsipras, Ludwig Schmidt, and Aleksander Madry. A rotation and a translation suffice: Fooling CNNs with simple transformations. *CoRR*, abs/1712.02779, 2017.
- [9] T. Gehr, M. Mirman, D. Drachler-Cohen, P. Tsankov, S. Chaudhuri, and M. Vechev. AI2: Safety and robustness certification of neural networks with abstract interpretation. In *2018 IEEE Symposium on Security and Privacy (SP)*, pages 3–18, May 2018.
- [10] Ian Goodfellow, Jean Pouget-Abadie, Mehdi Mirza, Bing Xu, David Warde-Farley, Sherjil Ozair, Aaron Courville, and Yoshua Bengio. Generative adversarial nets. In Z. Ghahramani, M. Welling, C. Cortes, N. D. Lawrence, and K. Q. Weinberger, editors, *Advances in Neural Information Processing Systems 27*, pages 2672–2680. Curran Associates, Inc., 2014.
- [11] Ian J. Goodfellow, Jonathon Shlens, and Christian Szegedy. Explaining and harnessing adversarial examples. *CoRR*, abs/1412.6572, 2014.
- [12] Kathrin Grosse, Nicolas Papernot, Praveen Manoharan, Michael Backes, and Patrick D. McDaniel. Adversarial perturbations against deep neural networks for malware classification. *CoRR*, abs/1606.04435, 2016.
- [13] Nikolaus Hansen. The CMA evolution strategy: A tutorial. *CoRR*, abs/1604.00772, 2005.
- [14] Nikolaus Hansen and Stefan Kern. Evaluating the CMA evolution strategy on multimodal test functions. In *PPSN*, 2004.
- [15] Nikolaus Hansen, Sibylle D. Müller, and Petros Koumoutsakos. Reducing the time complexity of the derandomized evolution strategy with covariance matrix adaptation (CMA-ES). *Evolutionary computation*, 11 1:1–18, 2003.
- [16] Andrew Ilyas, Logan Engstrom, Anish Athalye, and Jessy Lin. Query-efficient black-box adversarial examples. *CoRR*, abs/1712.07113, 2017.
- [17] Can Kanbak, Seyed-Mohsen Moosavi-Dezfooli, and Pascal Frossard. Geometric robustness of deep networks: analysis and improvement. *CoRR*, abs/1711.09115, 2017.
- [18] Jay B. Martin, Thomas L. Griffiths, and Adam Sanborn. Testing the efficiency of Markov chain Monte Carlo with people using facial affect categories. *Cognitive Science*, 36(1):150–162, 2012.
- [19] Matthew Mirman, Timon Gehr, and Martin Vechev. Differentiable abstract interpretation for provably robust neural networks. In *International Conference on Machine Learning (ICML)*, 2018.
- [20] Seyed-Mohsen Moosavi-Dezfooli, Alhussein Fawzi, and Pascal Frossard. DeepFool: A simple and accurate method to fool deep neural networks. In *CVPR*, pages 2574–2582. IEEE Computer Society, 2016.
- [21] Nina Narodytska and Shiva Prasad Kasiviswanathan. Simple black-box adversarial attacks on deep neural networks. *2017 IEEE Conference on Computer Vision and Pattern Recognition Workshops (CVPRW)*, pages 1310–1318, 2017.
- [22] Anh Mai Nguyen, Jason Yosinski, and Jeff Clune. Deep neural networks are easily fooled: High confidence predictions for unrecognizable images. In *IEEE Conference on Computer Vision and Pattern Recognition, CVPR 2015, Boston, MA, USA, June 7-12, 2015*, pages 427–436, 2015.
- [23] Nicolas Papernot, Patrick McDaniel, Ian Goodfellow, Somesh Jha, Z. Berkay Celik, and Ananthram Swami. Practical black-box attacks against machine learning. In *Proceedings of the 2017 ACM on Asia Conference on Computer and Communications Security - ASIA CCS 17*. ACM Press, 2017.
- [24] Nicolas Papernot, Patrick McDaniel, Somesh Jha, Matt Fredrikson, Z. Berkay Celik, and Ananthram Swami. The limitations of deep learning in adversarial settings. In *2016 IEEE European Symposium on Security and Privacy (EuroS&P)*. IEEE, mar 2016.
- [25] Nicolas Papernot, Patrick McDaniel, Somesh Jha, Matt Fredrikson, Z. Berkay Celik, and Ananthram Swami. The limitations of deep learning in adversarial settings. In *2016 IEEE European Symposium on Security and Privacy (EuroS&P)*. IEEE, mar 2016.
- [26] Mahmood Sharif, Lujo Bauer, and Michael K. Reiter. On the suitability of  $l_p$ -norms for creating and preventing adversarial examples. *CoRR*, abs/1802.09653, 2018.
- [27] Christian Szegedy, Wojciech Zaremba, Ilya Sutskever, Joan Bruna, Dumitru Erhan, Ian J. Goodfellow, and Rob Fergus. Intriguing properties of neural networks. *CoRR*, abs/1312.6199, 2013.
- [28] Rohan Taori, Amog Kamsetty, Brenton Chu, and Nikita Vemuri. Targeted adversarial examples for black box audio systems. *CoRR*, abs/1805.07820, 2018.
- [29] Matthew Wicker, Xiaowei Huang, and Marta Kwiatkowska. Feature-guided black-box safety testing of deep neural networks. In *Tools and Algorithms for the Construction and Analysis of Systems*, pages 408–426. Springer International Publishing, 2018.
- [30] Christian Wirth, Riad Akrou, Gerhard Neumann, and Johannes Fürnkranz. A survey of preference-based reinforcement learning methods. *Journal of Machine Learning Research*, 18:136:1–136:46, 2017.



(a)



(b)



(c)

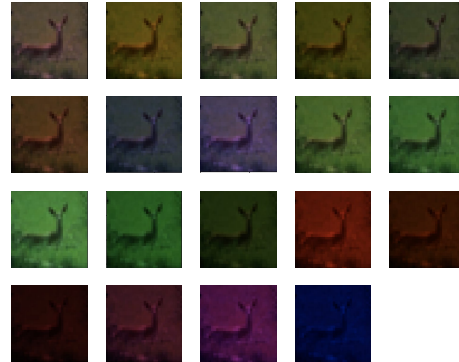


(d)

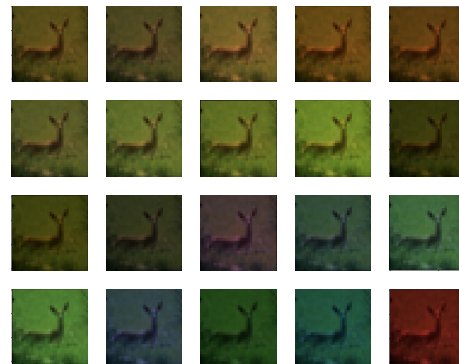
Fig. 9. Results of running CMA-ES using human perception for an example from GTSRB dataset; (a): Input image; (b): misclassified examples within the first iteration of CMA-ES run; (c): misclassified examples within the second iteration of CMA-ES run; (d): misclassified examples within the third iteration of CMA-ES run



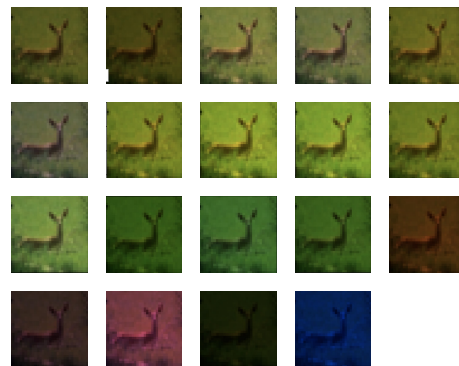
(a)



(b)



(c)



(d)

Fig. 10. Results of running CMA-ES using human perception for an example from CIFAR10 dataset; (a): Input image; (b): misclassified examples within the first iteration of CMA-ES run; (c): misclassified examples within the second iteration of CMA-ES run; (d): misclassified examples within the third iteration of CMA-ES run

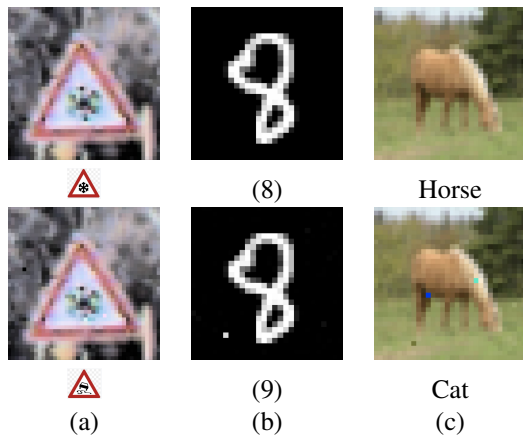


Fig. 11. Adversarial example generated by running human perception based CMA-ES; top: Legitimate samples from CIFAR10 dataset; bottom: Misclassified examples generated by CMA-ES for inputs from top row

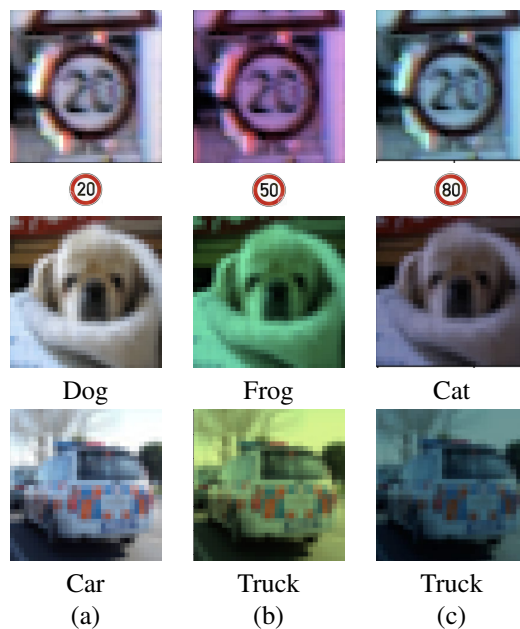


Fig. 13. Comparing  $L_1$  norm and human perception based adversarial example crafting, using color recombination; (a): original image; (b): adversarial example crafted using  $L_1$ ; (c) adversarial example crafted using human perception

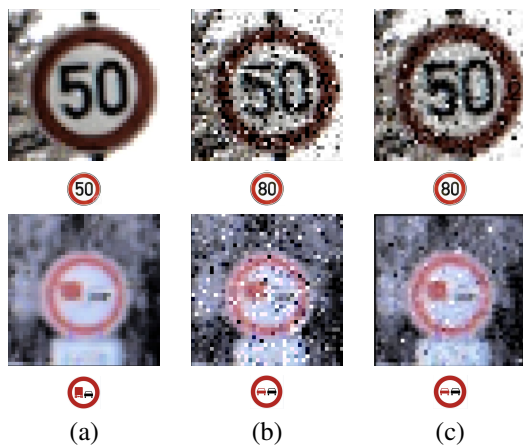


Fig. 12. Comparing  $L_1$  norm and human perception based adversarial example crafting, using pixel perturbation; (a): original image; (b): adversarial example crafted using  $L_1$ ; (c) adversarial example crafted using human perception